

**CdZnSe/Zn(Be)Se Quantum Dot Structures: Size, Chemical Composition and Phonons**

Y. Gu<sup>1</sup>, Igor L. Kuskovsky<sup>1</sup>, J. Fung<sup>1</sup>, R. Robinson<sup>1</sup>, I. P. Herman<sup>1</sup>, G. F. Neumark<sup>1</sup>, X. Zhou<sup>2</sup>, S. P. Guo<sup>2</sup>, and M. C. Tamargo<sup>2</sup>

<sup>1</sup>Department of Applied Physics & Applied Mathematics, Columbia University, New York, NY 10027

<sup>2</sup>Department of Chemistry, City College of CUNY, New York, NY 10031

**ABSTRACT**

The size and chemical composition of optically active CdZnSe/ZnSe and CdZnSe/Zn<sub>0.97</sub>Be<sub>0.03</sub>Se quantum dots (QDs) are determined using photoluminescence, photoluminescence excitation and polarized Raman scattering spectroscopies. We show that the addition of Be into the barrier enhances the Cd composition and the quantum size effect of optically active QDs. Additionally, surface phonons from QDs are observed in CdZnSe/ZnBeSe nanostructures.

**INTRODUCTION**

Self-assembled quantum dot (QD) systems have been of great interest due to both interesting physics and such promising applications as QD laser diodes and quantum computing. For optimum device performance, it is often necessary to have QDs with uniform size and chemical composition. However, due to inter-diffusion that usually occurs during the growth, the QDs obtained so far often have a relatively broad distribution in both size and chemical composition.

It is thus desirable to determine the specific size and chemical nature of the QDs that dominate the optical properties of the system. This has been attempted (see, e.g. [1]) by studying the photoluminescence (PL) of samples that are also characterized by transmission electron microscopy (TEM). However, such an approach is inconclusive since the QDs observed by TEM do not necessarily participate in optical processes (i.e. optically inactive).

In this paper, we show how to determine the size and chemical composition of optically active QDs directly from their optical properties. Specifically, we investigate PL, PL excitation (PLE) and Raman scattering properties, complemented by model calculations, and use CdSe/Zn(Be)Se QDs as an example. In addition, by comparing the results for the CdSe/ZnSe and CdSe/ZnBeSe systems, we show that the addition of Be into the barrier enhances the Cd composition of QDs as well as quantum size effect.

**RESULTS AND DISCUSSION**

In Figs. 1-(a) and (b) we plot the PLE as well as PL spectra of Cd<sub>x</sub>Zn<sub>1-x</sub>Se/ZnSe (sample A) and Cd<sub>x</sub>Zn<sub>1-x</sub>Se/Zn<sub>0.97</sub>Be<sub>0.03</sub>Se (sample B) QD structures, respectively. The PL spectra of both samples show a single relatively broad peak, whose energy depends on the size and Cd composition (x) of the optically active QDs. The PLE spectra for both samples are similar, showing free excitons from the barriers and broad features associated with the excitation via the wetting layers. In addition, the PLE spectrum from sample B (Fig. 1-(b)) also shows a small peak (not observed for sample A) separated from the detection energy (indicated by the arrow) by ~28meV. This type of feature is consistently observed across this sample's PL band; moreover, above 2.43eV up to three equally spaced peaks can be observed (not shown here). A closer look at this region (see the inset) reveals two peaks, which can be fitted well by Lorentzians. The energy differences between the detection energy and the Lorentzians are 29.0meV (peak 1) and 21.4meV (peak 2). The fitting has been carried out at several detection

energies across the PL peak, and the results are summarized in Table I. While peak 1 ( $\sim 28.7$ - $29.3$  meV) can be attributed to the CdZnSe QD LO phonons, peak 2 is below the bulk CdSe LO phonon energy (note that the ZnSe LO phonon energy is higher than CdSe) and therefore is likely due to a different origin. The absence of such a phonon-assisted excitation in sample A (Fig. 1-(a)) suggests a weaker phonon-exciton coupling, and therefore lower Cd composition and/or weaker quantum confinement in this sample [2].

To clarify the origin of the peaks observed in PLE and to obtain additional information about LO phonons in sample A, we performed room temperature (RT) polarized Raman scattering in configurations where only LO phonon scattering is allowed, using the 488nm and 514.5nm laser lines from an Ar<sup>+</sup> laser. The results are shown in Fig. 2 for sample A and Fig. 3 for sample B. The use of the 488nm line corresponds to the non-resonant case since there is no QD PL in this spectral region (see the insets); conversely, the 514.5nm line falls within the QD PL emission energies, corresponding to the resonant Raman scattering case. When the 488nm line is used (Figs. 2-(a) and 3-(a)) both samples show a GaAs LO phonon peak (also observed with 514.5nm laser line) at  $\sim 289\text{cm}^{-1}$  (35.8 meV) and a main peak with an asymmetric lineshape at  $\sim 250\text{cm}^{-1}$ . The latter was fitted with two Lorentzians (dashed lines) peaked at  $\sim 250\text{cm}^{-1}$  (31.0 meV) and  $243\text{cm}^{-1}$  (30.3 meV). We attribute the  $250\text{cm}^{-1}$  peak to Zn(Be)Se LO phonons. Following Ref. 3, we attribute the  $243\text{cm}^{-1}$  peak to interface phonons (IF) between the CdZnSe/Zn(Be)Se layers. Sample A shows an additional strong narrow peak at  $\sim 224\text{cm}^{-1}$  (27.8 meV). To identify this peak, we note that a wetting layer (WL) transition at  $\sim 2.56\text{eV}$ , which is very close to the 488nm (2.54 eV) laser line, has been previously observed by contactless electro-reflectance measurements [4]. Therefore, this  $224\text{cm}^{-1}$  peak can be attributed to the LO phonons in the WL, with the peak intensity being enhanced under the resonant condition (see Fig. 2-(a)).

The Raman spectra using the 514.5nm laser line (Figs. 2-(b) and 3-(b)) show some different features in comparison to the non-resonant case. First, for sample A (Fig. 2-(b)) the sharp  $224\text{cm}^{-1}$  peak disappeared as the laser line moved away from the energy of the WL transition, and a broad peak at  $\sim 228.3\text{cm}^{-1}$  (28.3 meV) shows up on the low energy side of the main peak. Considering that this broad peak only appears under the resonant condition, we attribute it to the CdZnSe QD LO phonons. For sample B (Fig. 3-(b)), one peak at  $\sim 227\text{cm}^{-1}$

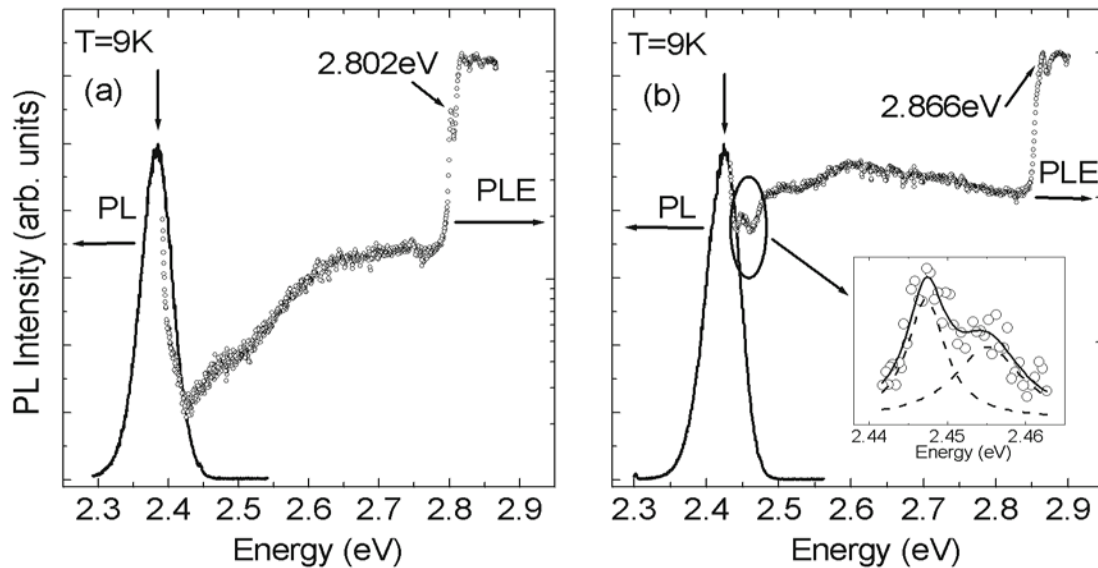


Fig. 1 The PL (solid lines) and PLE (circles) spectra of (a) sample A and (b) sample B. Arrows indicate the detection energies. The inset is the magnified marked region; the solid line is the fitting result using two Lorentzians (dashed lines).

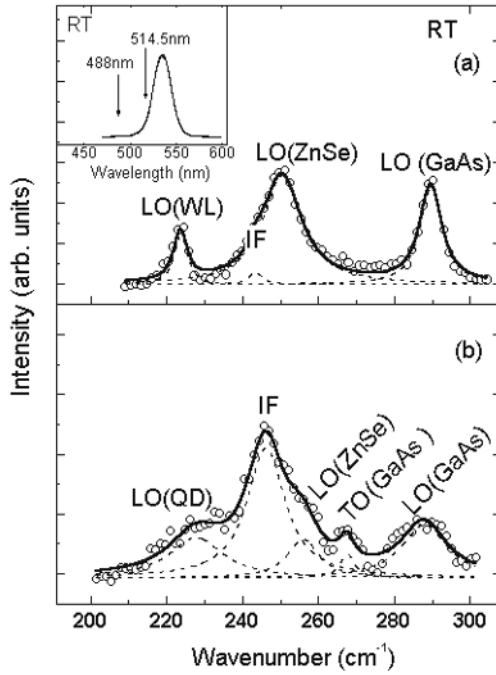


Fig. 2. The RT polarized Raman scattering for sample A using (a) the 488nm laser line; (b) the 514.5nm laser line (resonant with QDs RT PL; see the inset). Open circles are the experimental data; the solid line is the result of fitting with Lorentzians (dashed lines).

(28.1meV) and another peak at  $\sim 199\text{cm}^{-1}$  (24.6meV) are observed, neither of which is present in the non-resonant case discussed above. The energy of the former (latter) is very close to that of peak 1 (peak 2) observed in PLE. This leads us to the conclusion that both peaks have their origins in the QDs, with peak 1 due to LO phonons in the QDs. To understand the origin of peak 2, we note that its energy falls between the CdSe LO and TO phonon energies. Furthermore, similar peaks have been previously observed for CdSe QDs embedded in glass (see e.g. Refs. 5, 6 and references therein) and they have been attributed to surface (SF) phonons of QDs. Regarding previous observations of such peaks in self-assembled CdZnSe/ZnSe QDs (see, e.g. Ref. 7) in PLE, no clear identification was given. At this time we attribute this peak to CdZnSe QD SF phonons.

Since the QD LO phonon energies ( $\hbar\omega_{\text{LO}}$ ) are related to the size (see e.g. Ref. [8]) and chemical composition, one can obtain various combinations of QD size and Cd composition, each pair of which leads to the same given  $\hbar\omega_{\text{LO}}$ . The shapes of the QDs in sample A and sample B is assumed to be disk-type and spherical, respectively [9]. The details of calculations can be found elsewhere [10, 11]. In Fig. 4 we plot the results (the solid line) for sample B (spherical model) as an example. Every point on this curve corresponds to  $\hbar\omega_{\text{LO}} = 28.7\text{meV}$  with the coordinates of these points being size and Cd composition of QDs. It is obvious that no unique combination of QD size and Cd composition can be obtained based on the LO phonon energy alone. Another independent parameter, which has to be a function of QD size and composition, is therefore required. We note that from PLE, each  $\hbar\omega_{\text{LO}}$  is detected at one specific PL emission energy  $h\nu_{\text{det}}$ , both of which are characteristics of the same group of QDs, and  $h\nu_{\text{det}}$  can be indeed expressed as a function of QD size and Cd composition (within an appropriate model, for details see Refs. 10 and 11). The curve

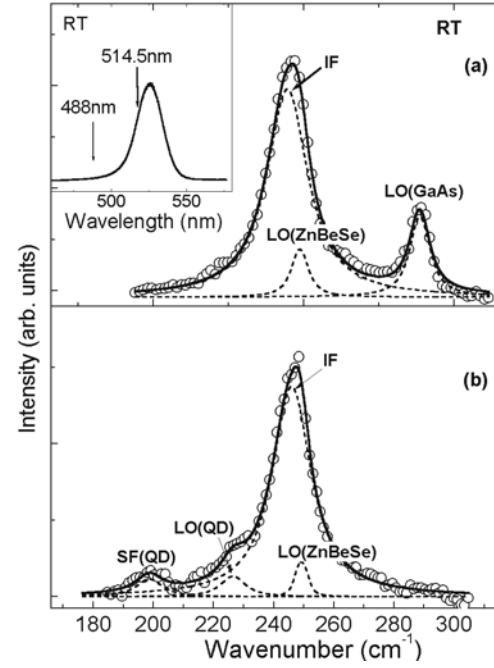


Fig. 3. The RT polarized Raman scattering for sample B using (a) the 488nm laser line; (b) the 514.5nm laser line (resonant with QDs RT PL; see the inset). Open circles are the experimental data; the solid line is the result of fitting with Lorentzians (dashed lines).

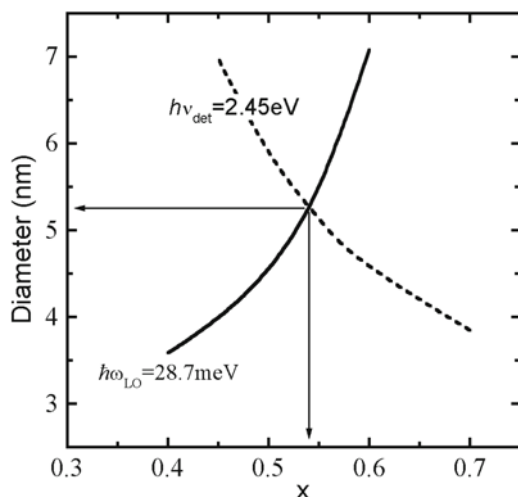


Fig. 4. Procedure for the determination of size and Cd composition of QDs in sample B (see also text).

representing  $h\nu_{\text{det}}$  for sample B (spherical model) is plotted in Fig. 4 (for calculation details, see Ref. 10). The intersection of these two curves then gives the unique combination of size and Cd composition of the QDs that emit at  $h\nu_{\text{det}}$ . The results for sample B are summarized in Table I.

For sample A, since no phonon-assisted excitation was observed through PLE, one can only consider the  $\hbar\omega_{\text{LO}}$  that corresponds to the photon energy of the 514.5nm laser line, which is in resonance with the QDs PL emission. Therefore, we are only able to obtain the size and Cd composition for one corresponding QD group. The disk model is used in this case with the radius/height ratio ( $\gamma=R/L_z$ ) taken to be 5 and 10. We note that for these two chosen ratios the final results are almost identical: for  $\gamma=5$ ,  $x=0.44$  and  $L_z=2.1\text{nm}$ ; for  $\gamma=10$ ,  $x=0.43$  and  $L_z=2.1\text{nm}$ .

In the same way, since the 488nm laser line is resonant with the WL emission, we can also obtain the Cd composition and thickness of the WL. For this sample we obtained 30%Cd and the thickness of  $\sim 1.65\text{nm}$ . It is important that the previous TEM studies on similar structures [12,13] gave the WL  $0.21 \leq x \leq 0.35$  and  $L_z$  of around 10ML ( $\sim 1.5\text{nm}$ ), in excellent agreement with our results.

Having obtained the size and composition of optically active QDs, we are then able to compare the results for these two samples. Ideally, it would be best to compare the results across the whole PL peak. However, such an approach is not feasible since no phonon peak could be detected from PLE for sample A. Nevertheless, as mentioned above, the absence of phonon peaks (meaning weaker exciton-phonon coupling) suggests a larger size and/or lower Cd composition of QDs in sample A. Furthermore, we note from Table I that the high energy side of the PL is dominated by smaller QDs with higher Cd compositions.

Table I. Estimated diameter and Cd composition (x) of QDs in sample B with corresponding LO and surface phonon energies.

$h\nu_{\text{det}}$ (eV)	Peak 1 (LO) (meV)	Peak 2 (SF) (meV)	x	Diameter (nm)
2.470	28.7	24.7	0.53	5.1
2.450	28.7	24.7	0.54	5.3
2.441	28.7	22.4	0.54	5.4
2.431	28.8	21.8	0.53	5.7
2.426	29.0	21.4	0.51	6.4
2.422	29.3	22.0	0.47	8.0
2.417	29.2	22.0	0.49	7.4

If this trend (QDs with higher Cd composition dominating the high-energy PL) is assumed for both samples, then the resultant Cd composition for sample A ( $x=0.43$ ) would represent the high end of the composition, which is lower than any  $x$  obtained for sample B (see Table I). In view of this, we thus suggest that the addition of Be into the barrier enhances the QDs' Cd composition. As to the QDs size, a comparison of the overall quantum size effect is more instructive since different models are used. As shown in Figs. 1-(a) and (b), the PL energy of sample A is lower than that of sample B. It is important that such a difference cannot be accounted for by the different barrier heights caused by the introduction of Be [14]. Moreover, higher Cd composition leads to lower bandgap energy, and thus sample B (with higher QD Cd composition) would emit PL at a lower energy than sample A if they had the same overall quantum size effect. The opposite case is observed here and thus clearly points to a stronger quantum size effect of QDs in sample B. Therefore, we conclude that Be also enhances the overall quantum size effect of optically active QDs.

## SUMMARY

In summary, we have investigated optical properties of CdSe/ZnBeSe and CdSe/ZnSe QDs using PL, PLE and Raman scattering spectroscopies. We have shown how to combine these with model calculations to estimate size and chemical composition of optically active QDs. Furthermore, using such an approach, we also have shown that the addition of Be into the barrier enhances the Cd composition and the overall quantum size effect of optically active QDs, and thus increases the LO phonon-exciton coupling in such QDs.

## ACKNOWLEDGEMENT

This work is supported in part by the MRSEC Program of the National Science Foundation under Award Number DMR-0213574 (R.R and I.P.H), the Ford Foundation (R.R), New York Science and Technology on Photonic Materials and Applications and Center for Analysis of Structures and Interfaces in CUNY (X.Z, S.P.G and M.C.T)

## REFERENCES

- [1] M. Strassburg, Th. Deniozou, A. Hoffmann, R. Heitz, U. W. Pohl, D. Bimberg, D. Litvinov, A. Rosenauer, D. Gerthsen, S. Schwedhelm, K. Lischka, and D. Schikora, *Appl. Phys. Lett.* **76**, 685 (2000).
- [2] D. V. Melnikov and W. B. Fowler, *Phys. Rev. B* **64**, 245320 (2001).
- [3] H. Rho, H. E. Jackson, S. Lee, M. Dobrowolska, and J. K. Furdyna, *Phys. Rev. B* **61**, 15641 (2000).
- [4] M. Munoz, S. P. Guo, X. Zhou, M. C. Tamargo, Y. S. Huang, C. Trallero-Giner, and A. H. Rodriguez, *Appl. Phys. Lett.* **83**, 4399 (2003)
- [5] M. C. Klein, F. Hache, D. Ricard, and C. Flytzanis, *Phys. Rev. B* **42**, 11123 (1990).
- [6] Y.-N. Hwang, S.-H. Park, and D. Kim, *Phys. Rev. B* **59**, 7285 (1999).
- [7] M. Lowisch, M. Rabe, F. Kreller, and F. Henneberger, *Appl. Phys. Lett.* **74**, 2489 (1999).
- [8] E. Roca, C. Trallero-Giner, and M. Cardona, *Phys. Rev. B* **49**, 13704 (1994).
- [9] Previous time-resolved PL studies [X. Zhou, M. C. Tamargo, S. P. Guo, and Y. C. Chen, *J. Electron. Mater.* **32**, 733 (2003)] show that the for sample A, the PL decay time increases with temperature, indicating a quasi-two-dimensional character; for sample B, the PL decay time stays constant with increasing temperature until  $T=150\text{K}$ , suggesting

zero-dimensional quantum confinement. Therefore, we consider the former to be spherical QDs and the latter to be quantum disks.

- [10] Y. Gu, Igor L. Kuskovsky, J. Fung, R. Robinson, I. P. Herman, G. F. Neumark, X. Zhou, S. P. Guo and M. C. Tamargo, *Appl. Phys. Lett.* **83**, 3779 (2003).
- [11] Y. Gu, Igor L. Kuskovsky, R. Robinson, I. P. Herman, G. F. Neumark, X. Zhou, S. P. Guo and M. C. Tamargo, to be submitted.
- [12] N. Peranio, A. Rosenauer, D. Gerthsen, S. V. Sorokin, I. V. Sedova, and S. V. Ivanov, *Phys. Rev. B* **61**, 16105 (2000).
- [13] D. Litvinov, D. Gerthsen, A. Rosenauer, H. Preis, E. Kurtz, and C. Klingshirn, *Phys. Stat. Sol (b)* **224**, 147 (2001).
- [14] Within the same model (sphere or disk), the change in the barrier bandgap ( $\sim 66\text{meV}$ ) results only in  $\sim 2\text{meV}$  difference in the PL energy.